Phase transition of traveling waves in bacterial colony pattern

Joe Yuichiro Wakano, Atsushi Komoto, and Yukio Yamaguchi
Department of Chemical System Engineering, The University of Tokyo, 7-3-1 Hongo, Bunkyo-Ku, Tokyo 113-8656, Japan
(Received 9 February 2003; published 12 May 2004)

Depending on the growth condition, bacterial colonies can exhibit different morphologies. Many previous studies have used reaction diffusion equations to reproduce spatial patterns. They have revealed that nonlinear reaction term can produce diverse patterns as well as nonlinear diffusion coefficient. Typical reaction term consists of nutrient consumption, bacterial reproduction, and sporulation. Among them, the functional form of sporulation rate has not been biologically investigated. Here we report experimentally measured sporulation rate. Then, based on the result, a reaction diffusion model is proposed. One-dimensional simulation showed the existence of traveling wave solution. We study the wave form as a function of the initial nutrient concentration and find two distinct types of solution. Moreover, transition between them is very sharp, which is analogous to phase transition. The velocity of traveling wave also shows sharp transition in nonlinear diffusion model, which is consistent with the previous experimental result. The phenomenon can be explained by separatrix in reaction term dynamics. Results of two-dimensional simulation are also shown and discussed.

DOI: 10.1103/PhysRevE.69.051904 PACS number(s): 87.18.Hf, 47.20.Hw, 87.23.Cc

I. INTRODUCTION

Cooperative self-organization of bacterial colonies has been intensively studied both experimentally and theoretically [1–8]. The series of these studies should be considered as a part of the large stream where we pursue the universal comprehension of pattern formation. One of the most impressive and illustrating way of study is to perform numerical calculation of nonlinear partial differential equations in multiple-dimensional space to show various beautiful patterns [9–14]. However, they are so complicated and it is very difficult to understand why a certain pattern is achieved only for appropriate parameters. Another effective way is to study a simple element extracted from the complicated system. In this study we focus on traveling wave solution (TWS) which is a very simple pattern formation in which a fix-shaped wave propagates at a constant velocity. TWS often exists even in the nonlinear reaction diffusion model which produces complicated pattern under appropriate condition. TWS is clearly one of the most important element of pattern formation and some analytical works have already been done on the study of bacterial colony pattern formation [15,16].

Cohen *et al.* reported that colony expanding velocity increased as the initial nutrient concentration increased in their experiment [3]. Moreover, they reported the sharp change in the functional form of velocity as a function of nutrient level. The function was discontinuous at the point where two-dimensional pattern changed. Although the observed two-dimensional colony growth was not simple traveling wave, this study implies that the discontinuous change of TWS might be the source of the pattern formation. If a traveling wave propagates at a constant velocity everywhere, the result should be simple disklike (two-dimensional) or spherelike (three-dimensional) pattern. Experimentally observed diverse spatial patterns imply that the propagating velocity or the form of interface varies depending on the local properties, e.g., curvature or nutrient concentration. If the system has two distinct TWSs both of which are quasistable but not globally stable, the spatial pattern in which the two TWSs are mixed might evolve. Discontinuous change of TWS is one of the keys which describes the formation of spatial patterns.

It is experimentally known that some bacterial strains belonging to the genus *Bacillus* or *Paenibacillus* produce very complicated and clear patterns, i.e., branching. One characteristic of the genus is the ability to sporulate. Spores are inactive and dormant state of cells, which can survive starvation or dry environment. Bacteria species with sporulation ability produce the complex patterns of spore distribution. Previous theoretical studies revealed that colony pattern is best understood when we consider the pattern as the history of active bacteria density. Spores are the history of bacteria activity and sporulation is an important process in which active bacteria density is recorded in the history. Many models of bacterial colony pattern formation assume sporulation, however, there are few experimental studies that measured the sporulation rate.

Mimura *et al.* suggested a model with linear diffusion and nonlinear reaction terms [14]. The model has the ability to reproduce four out of five observed patterns of bacterial colony. Mathematically, the ability comes from the separatrix in reaction term dynamics (a dynamical system where diffusion terms are neglected). As Mimura *et al.* describe in their paper, the model is constructed so that reaction term dynamics is an excitable system. When the global behavior of the trajectory discontinuously changes depending on the initial point (i.e., separatrix), this may produce very strong nonlinear effect. Biologically, however, separatrix in Mimura model is not very realistic. It assumes that sporulation rate is a decreasing function of nutrient and bacteria density. As sporulation is considered as adaptation to environmental deterioration, the rate is biologically expected to be high when nutrient density per bacterium is low, if it depends on bacteria density. Anyway, without the experimental data of sporulation rate, it is impossible to build a biologically reasonable model.

In this study, we first present the experimentally measured sporulation rate of bacteria as a function of the initial nutri-

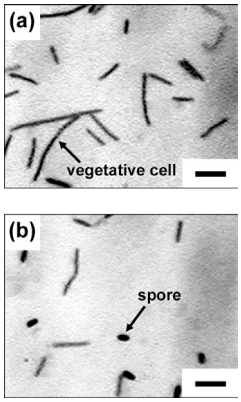

FIG. 1. Optical micrographs of *B. circulans* after 48 h incubation; (a) $N=0$ g/L and (b) $N=4.5$ g/L, respectively. Each scale bar indicates 5 μm. The arrows indicate a vegetative cell and a spore.

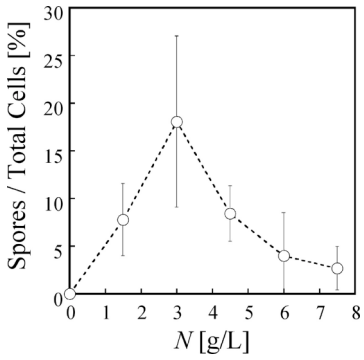

FIG. 2. The ratio of spores to total cells plotted vs the initial nutrient concentration. When nutrient concentration is very small, bacteria do not sporulate. $N=3.0$ g/L is best suited for sporulation.

ent. Due to the experimental difficulty, the quantitative relationship between sporulation rate and reproduction rate is unclear. The relationship can be qualitatively classified into three cases. Based on the experimental result, we propose three types of models. One of them has separatrix in its reaction term dynamics while the others do not. We perform one-dimensional computer simulations to study the existence of TWS and the dependence of the wave form and velocity on the initial nutrient concentration. Linear diffusion and nonlinear degenerate diffusion are studied. Results of two-dimensional simulation are also shown.

II. EXPERIMENTS AND RESULTS

In order to study sporulation rate, *Bacillus* bacteria were incubated in the liquid culture medium and the number of total cells and the ratio of spores were measured (Appendix A). Total density of both active (vegetative) cells and spores increased exponentially in the first 5 h (data not shown). This result is consistent with the previous work that the cell division of active bacteria is assumed to be a first-order reaction; $db/dt=kb$. Reaction rate coefficient k is estimated from the data of exponential growth stage. The dependence of k on the initial nutrient concentration N, well fits a well-known Michaelis-Menten-type function

$$k=\frac{k_{\max}C_N}{K+C_N},$$

where constant parameters are estimated as $k_{\max}=0.6$ h^{-1} and $K=2.2$ g/L, respectively.

We investigated the relationship between sporulation and the nutrient concentration. As sporulation is an adaptation to bad environmental conditions such as nutrient starvation or drying, sporulation rate has been considered as a decreasing function of nutrient concentration [14]. However, as shown in Fig. 1, few spores are formed under nutrient-free condition even after 48 h incubation. Thus we suppose that bacteria require some nutrient in order to sporulate. Biological knowledge of sporulation process supports the hypothesis [17]. In sporulation, DNA in a bacterial cell is replicated as in regular cell division. Inside the parent cell, one of them is coated with four-layered hard protein. The coated DNA is called a "forespore." After a forespore matures, the parent cell releases the forespore, which is called an "endospore" and can survive long periods of time in the bad environment. In short, as bacteria cannot replicate their DNA under nutrient-free condition, they cannot sporulate.

The ratio of spores to total cells was observed under the various initial nutrient concentration (Fig. 2). Predictably, few spores are formed at high nutrient level. The number of spores is highest when $N=3.0$ g/L. Although the ratio of spores is not equal to sporulation rate, the result strongly suggests that sporulation rate as a function of nutrient concentration has a single peak at a certain nutrient level.

Spores are observed about 23 h after the inoculation. By this duration sporulation rate is estimated to be much smaller than reproduction rate whose increasing time constant (doubling time) is estimated 1.0–1.5 h from the analysis of the growth curve in early stage. However, as long as the pattern dynamics of bacterial colony is concerned, spores are defined as inactive cells which cannot reproduce. As we could distinguish only endospores, it is presumable that time when vegetative cells transform into forespores is much earlier than the time of our observation [17]. So we measured the concentration of α-amylase in liquid culture, which is extracted by bacteria only when they sporulate into a forespore [18]. The drastic increase of α-amylase concentration (data not shown) suggests that formation of forespores occurs about 6–8 h after inoculation. The result implies that sporulation rate might be as large as reproduction rate for a certain interval of nutrient concentration. The result also implies that sporulation and germination process's take a long time and that no spore returned to the vegetative phase in our experiment. However, to evaluate the quantitative relationship between reproduction rate and sporulation rate, further experimental analysis is necessary.

III. MODELS AND RESULTS

A. Reaction term dynamics

First, we consider a model without spatial structure,

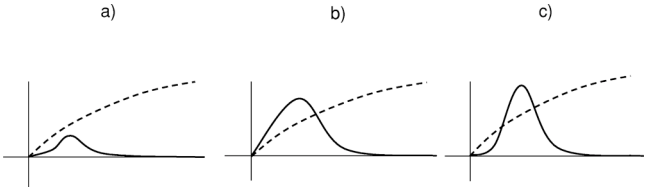

FIG. 3. Three possible models for the qualitative relationship of reproduction rate (dotted) and sporulation rate (solid).

$$\frac{db}{dt} = \alpha(n)b - \beta(n)b - \gamma b,$$

$$\frac{dn}{dt} = \alpha(n)b, \tag{1}$$

$$\frac{ds}{dt} = \beta(n)b,$$

where b, n, and s represent the density of active bacteria (vegetative cells), nutrient concentration, and the density of spores, respectively. $\alpha(n)$, $\beta(n)$, and γ correspond to reproduction rate, sporulation rate, and death rate, respectively. For simplicity, we assume that these rates do no depend on bacteria density. As for reproduction rate, Michaelis-Menten-type equation,

$$\alpha(n) = c_\alpha \frac{n}{n+1},$$

is known to be appropriate for various bacteria species. The natural death of the bacteria is not commonly observed. However, as spores are the special dormant state of bacteria, it is reasonable to assume that active bacteria cannot survive starvation. For simplicity, we assume the constant death rate of active bacteria, γ which is set to very low values compared to sporulation rate. The unit of bacteria concentration is rescaled so that nutrient conversion factor is 1. Our experiment suggests that sporulation rate is zero at $n=0,\infty$ and takes the maximum value at a certain nutrient concentration. Due to experimental difficulty, the quantitative relationship between sporulation rate and reproduction rate is unclear. Therefore, a large degree of freedom exists to determine the actual form of $\beta(n)$. Qualitatively, there are three possible relationships (Fig. 3): (a) sporulation is always slower than reproduction, (b) sporulation is faster than reproduction only when nutrient is poor, and (c) sporulation is faster than reproduction only for a certain interval of nutrient concentration.

In order to investigate the global behavior of these three models, we perform phase plane analysis. Vector field on (b,n) space is qualitatively determined, regardless of actual function form (Fig. 4). In models 1 and 2, it is obvious that the infinitesimal perturbation of the initial state only affects the terminal state infinitesimally. On the other hand, numerical calculation suggests that separatrix exists in model 3. When the initial nutrient concentration is lower than a critical value, all bacteria sporulate or die before nutrient is exhausted. When the initial nutrient concentration is higher than the critical value, almost all nutrient is consumed before active bacteria disappear. We present the mathematical proof of the existence of the critical value in Appendix B.

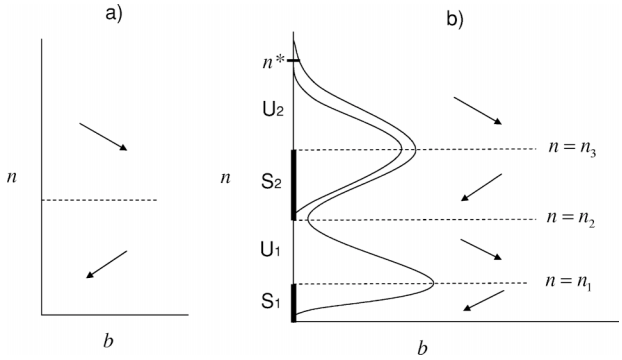

FIG. 4. The phase plane analysis of the models (see text). Dotted lines represent isoclines. (a) Models 1 and 2 have only one isocline and their vector fields are qualitatively the same. (b) Model 3 has three isoclines. Numerical calculation suggests the existence of separatrix around the critical initial value n^*. Two orbits starting from the initial values which are lower and higher than the critical value are shown.

We focus on the separatrix of model 3. It is natural to question whether the separatrix still exists when spatial diffusion is introduced. Furthermore, such a model may reproduce the observed sharp change of traveling wave velocity. The two-dimensional spatial pattern is also of great interest. These motivated us to construct a model with spatial structure based on model 3.

B. Linear diffusion model

First, we introduce linear diffusion

$$\frac{\partial b}{\partial t} = D\nabla^2 b + \alpha(n)b - \beta(n),$$

$$\frac{\partial n}{\partial t} = \nabla^2 n - \alpha(n)b, \tag{2}$$

where D represents diffusion coefficient of active bacteria. Some experimental knowledge is neglected for simplicity, such as nutrient chemotaxis or the dependence of bacterial activity on local nutrient concentration. Due to the simplification, D is constant and the model becomes easy to deal with. Under appropriate rescaling of time and space, diffusion coefficient of nutrient can be chosen as one without loss of generality. The density of spores s is dependent variable and is not analyzed here. We assume the sporulation rate to be a normal function:

$$\alpha(n) = c_\alpha \frac{n}{n+1},$$

$$\beta(n) = c_\beta \exp\{-\sigma(n-n_\beta)^2 + \gamma\}. \tag{3}$$

For the sake of simple notification, death rate is included in $\beta(n)$. Constant parameters $(c_\alpha, c_\beta, n_\beta, \gamma)$ are chosen so that a

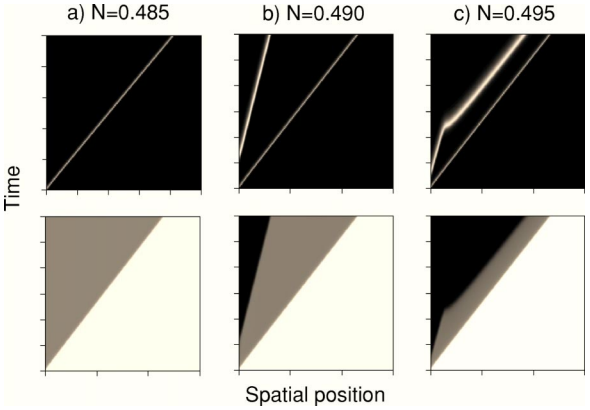

FIG. 5. Results of the numerical calculation of linear diffusion model ($D=1$). The spatiotemporal patterns of bacteria (upper row) and nutrient (lower row) are shown. Horizontal and vertical axes correspond to spatial position and time, respectively. Brightness represents density (concentration) of bacteria (nutrient), scales of which are kept constant. (a) $N=0.485$, (b) $N=0.490$, and (c) $N=0.495$.

model corresponds to model 3 in the preceding section. In all numerical calculations, we put $(c_\alpha, c_\beta, n_\beta, \gamma) = (0.3, 0.1, 0.3, 0.01)$.Crank-Nicholson scheme is applied to calculate diffusion term with zero flux boundary condition. Initially, nutrient is uniformly distributed at a level N and the small amount of active bacteria are put at the origin while no spore is present.

As a result of numerical simulation of the model in one-dimensional space, traveling wave is formed for most initial conditions. However, we found interesting behavior for a certain small parameter region (Fig. 5). When N is smaller than the critical value N^*, a bacterial wave has a single peak [Fig. 5(a)]. When N is larger than N^*, a new wave appears behind the original wave [Fig. 5(b)]. A wave in the back propagates initially slower, but when the distance between two waves reaches a certain value, a wave in the back begins to propagate at the same velocity as the fore wave. In other

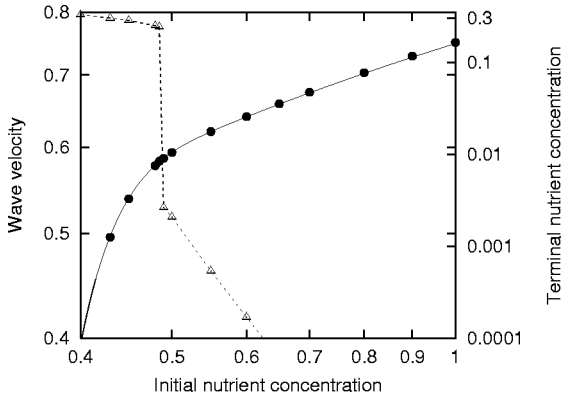

FIG. 6. Velocity of traveling wave (circle), velocity of that in the linearized system (bold line), and nutrient concentration left behind the wave (triangle) are shown against the initial nutrient concentration. The phase transition of the wave form occurs at the critical initial nutrient concentration while the wave velocity changes continuously and smoothly, $D=1$.

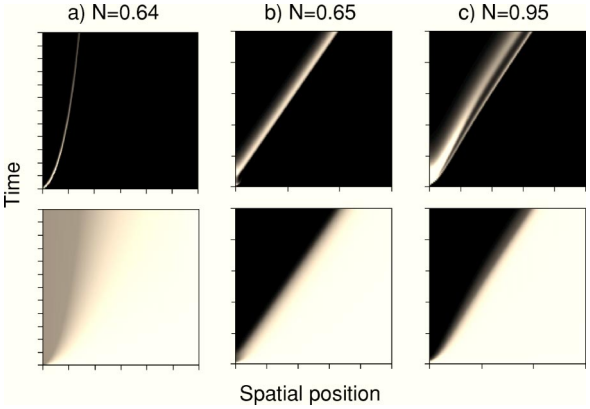

FIG. 7. Results of numerical calculation of nonlinear diffusion model ($D=1$). Scales are different for each N. (a) $N=0.64$, (b) $N=0.65$, and (c) $N=0.95$.

words, a wave becomes twofold [Fig. 5(c)]. Moreover, at the same critical value N^*, nutrient concentration left behind the wave sharply changes (from 0.24 to 0.0026). This critical initial value N^* is estimated as $0.485 < N^* < 0.49$. The result suggests that according to the initial condition this system have two phases, a singlefold traveling wave leaving some amount of nutrient behind and a twofold traveling wave leaving little nutrient behind. We conclude that the separatrix in reaction term dynamics is maintained against introduction of linear diffusion.

Surprisingly, however, propagating velocity does not show sharp change (Fig. 6). To guess the velocity analytically, we derive the linear spreading velocity of b in the linearized equation about the unstable state $(b,n)=(0,N)$ [19],

$$\frac{\partial b}{\partial t} = D\nabla^2 b + Sb,$$

$$\frac{\partial n}{\partial t} = \nabla^2 n - \alpha(N)b, \tag{4}$$

$$S = \alpha(N) - \beta(N),$$

in which the first equation is the linearized Fisher-Kolmogoroff equation whose linear spreading velocity c is

$$c = \sqrt{SD}, \tag{5}$$

when the initial condition has a compact support. The numerical calculation shows that the velocity of TWS in the nonlinear model [Eq. (2)] is equal to the linear spreading velocity (Fig. 6). This means that the wave has a "pulled front" in the sense that the global nonlinear dynamics of the traveling wave is governed by the dynamics around the leading edge where the linearized system is a good approximation [19]. This might be the reason why the velocity is a continuous function of the initial nutrient concentration despite the existence of the separatrix in reaction term dynamics.

C. Nonlinear diffusion model

Nonlinear diffusion coefficient has been first applied to bacterial colony pattern problem by Kawasaki *et al.* [10]. Biologically, such diffusion is considered as a result of cooperative cell motion. There are several evidences of cell-cell signal exchange and it is natural to consider that bacterial diffusion is not simple linear diffusion of bacteria. Mathematically, the following Fisher-Kolmogoroff equation with nonlinear diffusion is well studied:

$$\frac{\partial u}{\partial t} = \nabla (D(u) \nabla u) + u(1-u). \tag{6}$$

When $D(u)=u$, a complete analysis has been carried out [20–22] while more general problems are also intensively studied [15,23–25]. When $u=0$, the diffusion term vanishes and the equation degenerates into an ordinary differential equation. So this type of equation is often referred to as nonlinear degenerate parabolic equation. In relation to singularity of $u=0$, a characteristic solution is known in this system. The TWS $u(x,t)=U(x-ct)=U(z)$ satisfying

$$U(-\infty)=1, \quad U(z)=0 \quad \forall\, z \geqslant z^*, \quad U'(z^*) \neq 0, \quad z^* < +\infty$$

is called as the TWS of sharp type. In this solution, $u=0$ in front of the wave front ($z \geqslant z^*$) while $u>0$ behind the front ($z<z^*$). In the linear diffusion equation, on the other hand, u only approaches zero as $z \to \infty$. The TWS of sharp type is known to exist in models with various reaction terms and nonlinear degenerate diffusion term.

We focus on the property of the sharp wave front. The preceding discussion of linear conjecture of wave velocity does not hold in such TWS. Therefore, the wave velocity as a function of the initial nutrient concentration may change sharply as the wave form does. In order to keep the model as simple as possible, we introduce nonlinear diffusion coefficient of bacteria, which is a function of only bacteria density. We will study the following equations:

$$\frac{\partial b}{\partial t} = D \nabla (b \nabla b) + \alpha(n) b - \beta(n),$$
$$\frac{\partial n}{\partial t} = \nabla^2 n - \alpha(n) b, \tag{7}$$

and perform numerical calculation of the model in one-dimensional space. We will use the same $\alpha(n)$ and $\beta(n)$ [Eq. (3)].

As a result of computer simulation, traveling wave is always formed (Fig. 7). The separatrix of the wave form remains. Nutrient concentration left behind the wave front sharply changes at the critical value $N_1^* \simeq 0.64$. However, a wave form remains single wave until N exceeds another critical value $N_2^* \simeq 0.93$. Above the critical value, a wave form becomes twofold. As is discussed, we are interested in the asymptotic behavior of the wave front. Global wave form and the detail of the wave front of typical twofold waves in linear and nonlinear diffusion models are shown in Fig. 8. The wave front of the linear diffusion model is smooth while that of the nonlinear diffusion model is sharp, convex, and

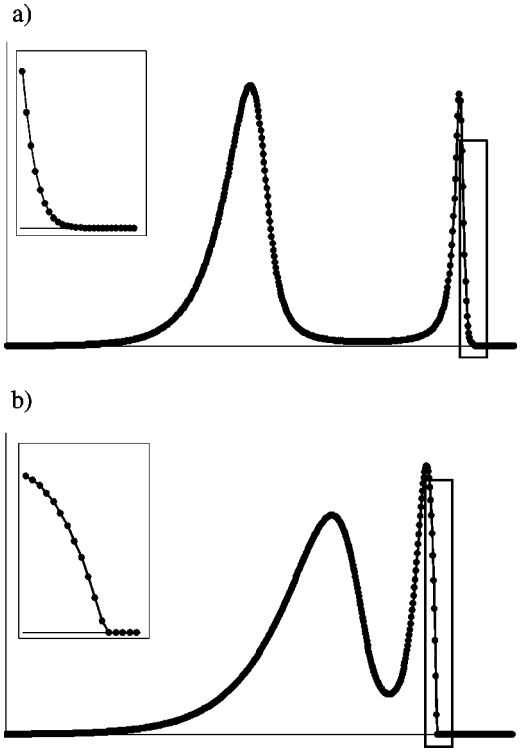

FIG. 8. Wave form of bacteria density in the (a) linear and (b) nonlinear diffusion models ($D=1$). Enlarged figures show that the front is smooth in the linear diffusion model and sharp in the nonlinear diffusion model. (a) $N=0.495$ and (b) $N=0.95$.

intersects $b=0$ line. It is confirmed that all TWSs in the linear diffusion model are of smooth type and that all TWSs in the nonlinear diffusion model are of sharp type. As is expected from these facts, wave velocity showed sharp change at both initial conditions where wave form sharply changes [Fig. 9(a)]. Notice the remarkable similarity between this and the experimental result of the colony growth velocity of *Paenibacillus dendritiformis* bacteria [Fig. 9(b)], although in the experiment the growth velocity of complicated two-dimensional pattern was measured. Another interesting point is that two types of phase transition, which occur at the same time in the linear diffusion model, occur independently. At the present state, however, we have no analytical explanation why two different critical values appear.

D. Two-dimensional simulation

In order to study the effect of the phase transition of wave form and velocity in a two-dimensional version of the model, we performed numerical calculation. Preliminary simulation showed that the linear diffusion model [Eqs. (2) and (3)] does not show any structured pattern other than simple disklike pattern. So we focus on the nonlinear diffusion model [Eqs. (3) and (7)]. The density of spores s is calculated as

$$\frac{ds}{dt} = c_\beta \exp\{-\sigma(n-n_\beta)^2\}. \tag{8}$$

Owing to limited computer time, calculation was done in the positive quadrant divided into 2000×2000 square lattices.

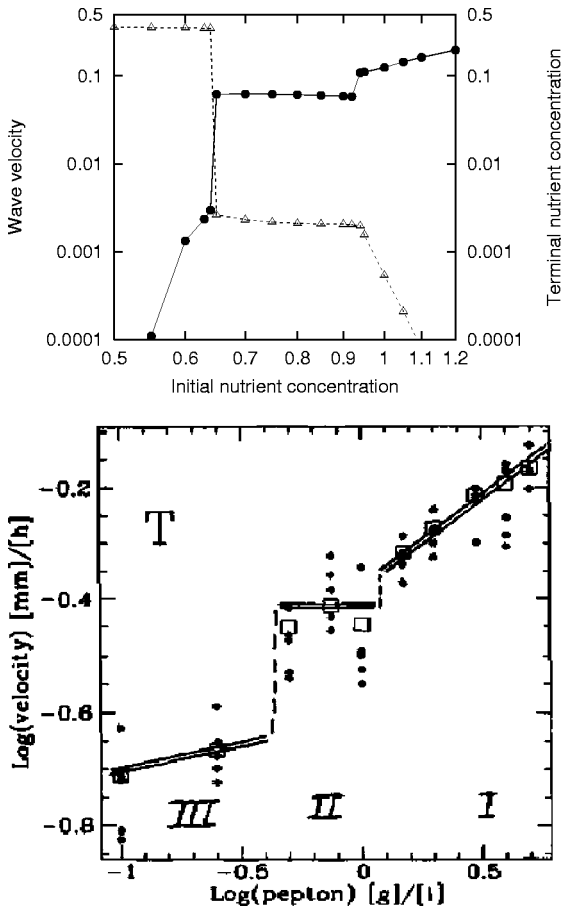

FIG. 9. (a) Velocity of traveling wave (circle) and nutrient concentration left behind the wave (triangle) are shown against the initial nutrient concentration. The phase transition of both the wave form and the velocity occurs, $D=1$. (b) Experimentally observed colony growth velocity. Reprinted from Ref. [3], Copyright (2004), with permission from Elsevier.

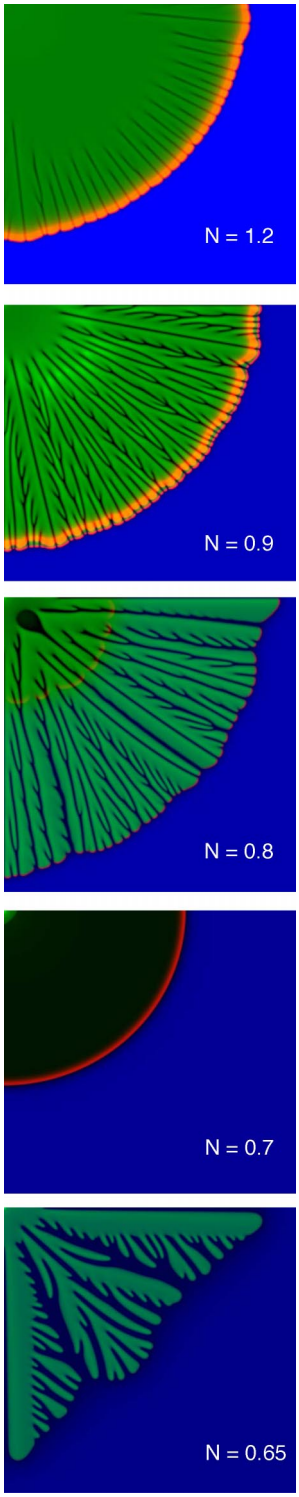

FIG. 10. Results of two-dimensional simulation of nonlinear diffusion model ($D=1$). Spatial distribution of $b+s$ is shown. The brightness of b is expressed five times stronger than that of s. Except $N=0.7$, a branching pattern is formed. A small amount of nutrient is left behind the front when $N=0.65$.

The response of the pattern to the initial nutrient concentration N is studied (Fig. 10). As a result, four typical patterns are obtained; namely, fine branching, ring, branching, and dense finger. When N is very low, fine branching pattern is observed. This pattern is also similar to dense-branching morphology (DBM) pattern. In experiments, both fine branching and DBM are observed when the initial nutrient is low, which is consistent with the present numerical result [3,26].

When N exceeds the first critical value $N_1^* \simeq 0.66$, the whole pattern changes very sharply. Nutrient concentration left behind changes from 0.35 to 0.002 and the pattern itself also changes to ring pattern. The corresponding transition in one-dimensional simulation has been already described in the preceding section. The result means that the separatrix originating from the reaction term still remains in two-dimensional model with nonlinear diffusion. In the ring pattern, no spore is left behind the bacterial front. There is no experimental observation which supports this. However, the phase transition of two-dimensional pattern is mathematically interesting.

When N exceeds the second critical value $N_2^* \simeq 0.78$, the pattern changes into branching pattern. This change is also very sharp, suggesting that it is another separatrix. It seems that there are two independent traveling waves of bacteria. Only forward wave produces branching pattern and back

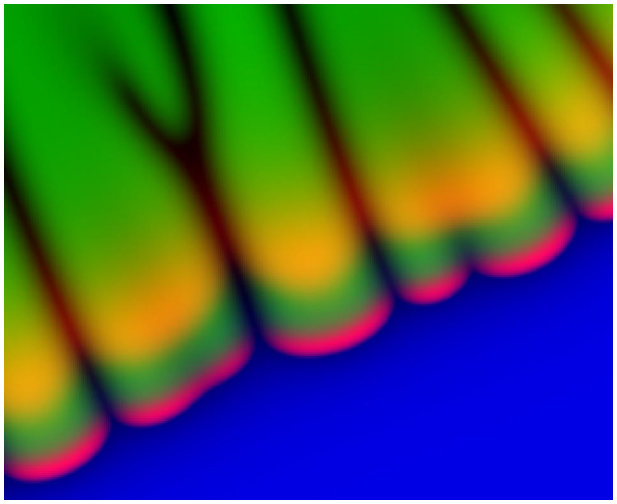

FIG. 11. Enlarged figure of two-dimensional branching pattern when $N=0.9$.

wave, propagating at slower speed, contributes little to the global pattern.

When N exceeds the third critical value $N_3^* \simeq 0.89$, the two bacterial waves are combined to form the twofold wave, while the global pattern does not change very much. Enlarged pattern is shown in Fig. 11. Singlefold and twofold waves are mixed along the front line. Twofold wave in bacterial pattern corresponds to the tip of the growing branch in spore pattern. Twofold wave consists of a fore wave corresponding to the first positive region of net bacterial reproduction rate where nutrient is high ($n > n_3$) and a back wave corresponding to the second region where nutrient is low ($n_1 < n < n_2$) [Fig. 4(b)]. Spores are produced in the region $n_2 < n < n_3$ while bacteria simply die out in the region $n < n_1$. Therefore, most spores are left behind the fore wave, which only the twofold wave has.

When N is increased further, the pattern gradually changes into dense fingering. In experiments, dense fingering pattern is observed when the initial nutrient is high, too. In our model, the change is caused by increase in twofold wave region in the front line.

There is no unique method to measure the growth velocity of such complex patterns. When we roughly estimate the velocity as a function of the initial nutrient, it is similar to the result of one-dimensional model. The velocity is very slow when $N < N_1^*$, almost the same when $N_1 < N < N_2^*$, and then increases rapidly when $N > N_3^*$.

Generally, in branching pattern formation, active spot exists only at the tip of growing branch. The possible mechanism for such spatiotemporal pattern formation is as follows. First, simple disklike pattern (radial traveling wave solution) becomes unstable due to some nonlinearity in the model. Such interface instability has been well studied, e.g., Mullins-Sekerka dispersion relation in crystal growth theory. In the particular field of bacterial colony growth, the interface instability of a simple nonlinear model is intensively studied [16,27]. Dispersion relation, however, only provides the most unstable wave number and its stability. In order to form clear pattern, active spot should be independent distinct aggregate. It has been unclear why wave front evolves to active and inactive parts which are so clearly distinguishable.

Based on the existence of separatrix, we here propose a hypothesis why clear patterns are observed in our model. From our calculation on the one-dimensional space, it is naturally expected that the model potentially has two types of stable states, i.e., a singlefold TWS and a twofold TWS. The initial condition determines which is realized. Transition between these states is discontinuous, i.e., separatrix. When the model is extended to the two-dimensional version, global TWS may become unstable under some condition. In such case, spatial heterogeneity may evolve into the mixture of singlefold and twofold waves, both of which are locally stable in so small region that the system is approximately equal to the one-dimensional model in radial direction. The length of the region along the front line might be determined by dispersion relation analysis. Separatrix originating from the reaction term produces two distinct areas in the wave front, which moves outward to draw clear branching pattern.

IV. CONCLUSION

We performed an experiment to determine the sporulation rate as a function of the nutrient concentration. Based on the result, a reaction diffusion model of bacterial colony growth is proposed. Especially, we focus on separatrix in reaction term dynamics. We study the effect of separatrix on traveling wave solution to find a different behavior; transition between a singlefold and a twofold wave. The phase transition of the velocity of the traveling wave shows great similarity with the previous experiment. Results of a two-dimensional simulation of our model are generally consistent with the observed patterns.

In our model with $N > N_2^*$, the spatial pattern of spores shows clear branching while that of bacteria does not. This seems inconsistent with the observed patterns, which should be studied in future. The effect of the diffusion coefficient of nutrient, the elimination of the effect of square lattice in numerical calculation, and the mathematical proof or the explanation of separatrix in reaction diffusion equation are also open problems.

As we mentioned at the beginning of the paper, the study of bacterial colony growth is not only a special biological topic but also it must be an attempt to explore universal law of pattern formation. Good theoretical study suggests new biological experiments while a new biological result inspires new models. Although bacteria are one of the simplest form of life, they produce so complex patterns. We hope the present study contribute to our comprehension of self-organized pattern formation.

APPENDIX A: EXPERIMENTAL METHOD

There are some *Bacillus* species each of which produces the original colony patterns. We used *Bacillus circulans* (*B. circulans*) as a spore forming species, but the qualitative features of sporulation learned in one species can be applied to another. *B. circulans* was incubated in the liquid culture medium which was prepared by the following methods [28].

10 g/L sodium chloride and nutrients with various concentration were dissolved in distilled water. We used Bacto Tryptone Peptone (TP) and Bacto Yeast Extract (YE) as nutrients, which contain vitamin, amino acid, minerals, and carbon sources. They were purchased from Difco, Detroit, M1, USA. The weight ratio was kept TP/YE=2 and the initial total concentration N was varied from 0 g/L to 15 g/L. This solution was autoclaved for 15 min at 120°C and 2 atm and then cooled down to room temperature. Bacteria, which had been stored at −20°C to prevent them from mutation, were preincubated in this liquid culture with N=15 g/L. After 15–18 h preincubation, bacteria density became about 10^8 -10^9 number/mL while no spore was formed. The bacteria density was adjusted to about 10^7 number/mL and then constant quantity of the solution was incubated in a plastic tube filled with fresh liquid culture. The tube was let in the bath incubator whose temperature was controlled at 37°C and shaken during incubation. We adopted batch-type incubation, in which fresh nutrient was not fed during incubation.

We took 5 μL of test portion from each liquid culture after 30 h incubation. The total bacteria number in each test portion was counted by using Thoma blood cell counter and an optical microscope (×400) and then the bacteria density was calculated. The ratio of spores to total cells was analyzed by the following method. Bacteria in every test portion were stained by Möller's spore staining method for the easy optical microscopic observation. Optical micrographs (×1000) of every sample were taken by a digital camera. In the micrographs, spores and vegetative cells are easily distinguishable. The ratio of spores were calculated by imaging software.

APPENDIX B: EXISTENCE OF SEPARATRIX

We consider a dynamical system

$$\frac{db}{dt} = \alpha(n)b - \beta(n)b,$$
$$\frac{dn}{dt} = -\alpha(n)b, \tag{B1}$$

defined in the positive quadrant $R_+^2=\{(b,n): b\geqslant 0, n\geqslant 0\}$. We assume $\alpha(0)=0$ which guarantees any orbit remains in R_+^2. The set of equilibrium points of Eq. (B1) is n axis ($b=0$). We assume continuous functions $\alpha(n)$ and $\beta(n)$ satisfy

$$0 < \alpha(n) < A \;\forall\; n > 0, \tag{B2}$$

$$0 < \beta_1 < \beta(n) < \beta_2, \tag{B3}$$

and thus n is monotonically decreasing function of t. Therefore, chaos or limit cycle never occurs. Apparently, n cannot diverge so we focus on whether b diverges or not. As long as $b>0$, n decreases. When $n=0$, $db/dt<-\beta_1 b$ holds, which means b converges to zero. Therefore, all orbits converge to the equilibrium points on n axis.

Eigenvalues of linear analysis around an equilibrium point $(0,n)$ on n axis are

$$\lambda = 0, S \tag{B4}$$

and

$$S \equiv \alpha(n) - \beta(n), \tag{B5}$$

with eigenvectors

$$\begin{pmatrix} 0 \\ 1 \end{pmatrix} \quad \text{and} \quad \begin{pmatrix} S \\ -\alpha(n) \end{pmatrix},$$

respectively. The zero eigenvalue means that the equilibrium points are neutrally stable against perturbation in a n axis direction, which is trivial because whole n axis is equilibrium. The sign of S determines whether an equilibrium is a repeller or an attractor.

Here we assume the qualitative relationship between $\alpha(n)$ and $\beta(n)$ is the same as in model 3 in text. According to the stability, n axis is divided into four subsets; stable line segment $S_1(0<n<n_1)$, unstable line segment $U_1(n_1<n<n_2)$, stable line segment $S_2(n_2<n<n_3)$, and unstable half line $U_2(n_3<n)$ [Fig. 4(b)]. As n is monotonically decreasing, any orbit starting from U_1 must enter S_1. Let $f(p)$ as a terminal point of an orbit starting from a point p. According to $f(p)$, U_2 consists of the following two subsets:

$$U_{21} \equiv \{p \in U_2 : f(p) \in S_1\}, \tag{B6}$$

$$U_{22} \equiv \{p \in U_2 : f(p) \in S_2\}. \tag{B7}$$

As we proved, any orbit converges to the equilibrium and

$$U_2 = U_{21} \cup U_{22}, \tag{B8}$$

$$U_{21} \cap U_{22} = \phi, \tag{B9}$$

hold. Hereafter, we prove the following theorem.

Theorem 1. (existence of separatrix). There exists unique $N^*>n_3$ such that

$$U_{21} \supseteq \{(0,n) \in U_2 : n > N^*\},$$

$$U_{22} \supseteq \{(0,n) \in U_2 : n_3 < n < N^*\}.$$

Proof. It is geometrically apparent that both U_{21} and U_{22} are connected because phase plane is two dimensional and any two orbits never intersect each other. Apparently, U_{21} must be above U_{22} on n axis; otherwise there should be intersecting orbits. The theorem is proved if $U_{21} \neq \phi$ and $U_{22} \neq \phi$ are proved.

Inclination of an orbit

$$\frac{db}{dn} = \frac{\alpha(n) - \beta(n)}{\alpha(n)}$$

is bounded for $n > n_2$ because α and β are bounded and because $\alpha > 0$ for $n > n_2$. Thus, b can change infinitesimally with infinitesimal change of n. Moreover, $db/dn \neq 0$ for $n \neq n_3$. This means that $|f(p) - p_3| < O(\epsilon)$ if $|p - p_3| < \epsilon$, where $p_3 \equiv (0, n_3)$. In other words, an orbit starting from a point infinitesimally above p_3 must enter a point infinitesimally below p_3, which is an element of S_2. Thus, $U_{22} \neq \phi$.

When $p \to (0, \infty)$, the orbit starting from p intersects $n = n_3$ line at (∞, n_3) as $db/dn > 0$ for $n > n_3$. However, decrease in b is finite in finite interval $[n_2, n_3]$ as inclination of the orbit is finite. Thus, the orbit starting from a point with very large n must enter S_1, which means $U_{21} \neq \phi$.□

[1] E. O. Budrene and H. C. Berg, Nature (London) **349**, 630 (1991).
[2] E. O. Budrene and H. C. Berg, Nature (London) **376**, 49 (1995).
[3] I. Cohen, A. Czirok, and E. Ben-Jacob, Physica A **233**, 678 (1996).
[4] I. Cohen, I. G. Ron, and E. Ben-Jacob, Physica A **286**, 321 (2000).
[5] J. Y. Wakano, S. Maenosono, A. Komoto, N. Eiha, and Y. Yamaguchi, Phys. Rev. Lett. **90**, 258102 (2003).
[6] N. H. Mendelson and J. Lega, J. Bacteriol. **180**, 3285 (1998).
[7] N. H. Mendelson, A. Bourque, K. Wilkening, K. R. Anderson, and J. C. Watkins, J. Bacteriol. **181**, 600 (1999).
[8] A. Komoto, K. Hanaki, S. Maenosono, J. Y. Wakano, Y. Yamaguchi, and K. Yamamoto, J. Theor. Biol. **225**, 91 (2003).
[9] E. Ben-Jacob, O. Schochet, A. Tenenbaum, I. Cohen, A. Czirok, and T. Vicsek, Nature (London) **368**, 46 (1994).
[10] K. Kawasaki, A. Mochizuki, M. Matsushita, T. Umeda, and N. Shigesada, J. Theor. Biol. **188**, 177 (1997).
[11] M. Matsushita, J. Wakita, H. Itoh, I. Rafols, T. Matsuyama, H. Sakaguchi, and M. Mimura, Physica A **249**, 517 (1998).
[12] I. Golding, Y. Kozlovsky, I. Cohen, and E. Ben-Jacob, Physica A **260**, 510 (1998).
[13] Y. Kozlovsky, I. Cohen, I. Golding, and E. Ben-Jacob, Phys. Rev. E **59**, 7025 (1999).
[14] M. Mimura, H. Sakaguchi, and M. Matsushita, Physica A **282**, 283 (2000).
[15] R. A. Satnoianu, P. K. Maini, F. S. Garduno, and J. P. Armitage, Discrete Contin. Dyn. Syst., Ser. B **1**, 339 (2001).
[16] J. Muller and W. van Saarloos, Phys. Rev. E **65**, 061111 (2002).
[17] C. Woese, *Microbiology* (Saunders, Orland, 1997).
[18] W. L. Nicholson and G. H. Chambliss, J. Bacteriol. **161**, 875 (1985).
[19] W. van Sarloos, Phys. Rep. **386**, 29 (2003).
[20] D. G. Aronson, *Density-Dependent Iinteraction-Systems* (Academic Press, New York, 1980).
[21] W. I. Newman, J. Theor. Biol. **85**, 325 (1980).
[22] J. D. Murray, *Mathematical Biology* (Springer, New York, 1989).
[23] W. I. Newman, J. Theor. Biol. **104**, 473 (1983).
[24] F. Sanchez-Garduno and P. K. Maini, J. Math. Biol. **33**, 163 (1994).
[25] Y. Hosono, Jpn. J. Ind. Appl. Math. **3**, 163 (1986).
[26] U. W. Wakita, K. Komatsu, A. Nakahara, T. Matsuyama, and M. Matsushita, J. Phys. Soc. Jpn. **63**, 1205 (1994).
[27] S. Kitsunezaki, J. Phys. Soc. Jpn. **66**, 1544 (1997).
[28] N. Eiha, A. Komoto, S. Maenosono, J. Y. Wakano, K. Yamamoto, and Y. Yamaguchi, Physica A **313**, 609 (2002).